Accepted Manuscript

T-shaped D−π−A−(π−A)$_2$ chromophores with two auxiliary electron acceptors

Parmeshwar Solanke, Oldřich Pytela, Filip Bureš, Milan Klikar

Please cite this article as: Solanke P, Pytela Oldř, Bureš F, Klikar M, T-shaped D−π−A−(π−A)$_2$ chromophores with two auxiliary electron acceptors, *Dyes and Pigments* (2018), doi: https://doi.org/10.1016/j.dyepig.2018.10.077.
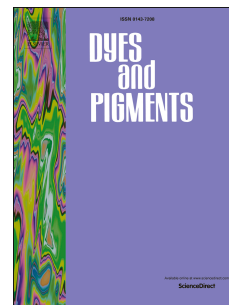
T-shaped D−π−A−(π−A)₂ Chromophores with Two Auxiliary Electron Acceptors

Parmeshwar Solanke,[a] Oldřich Pytela,[a] Filip Bureš,[a] and Milan Klikar*[a]

[a] Institute of Organic Chemistry and Technology, Faculty of Chemical Technology,

University of Pardubice, Studentská 573, Pardubice, 532 10, Czech Republic. Email:

Milan Klikar - milan.klikar@upce.cz (Web: http://bures.upce.cz/klikar.html)

TOC
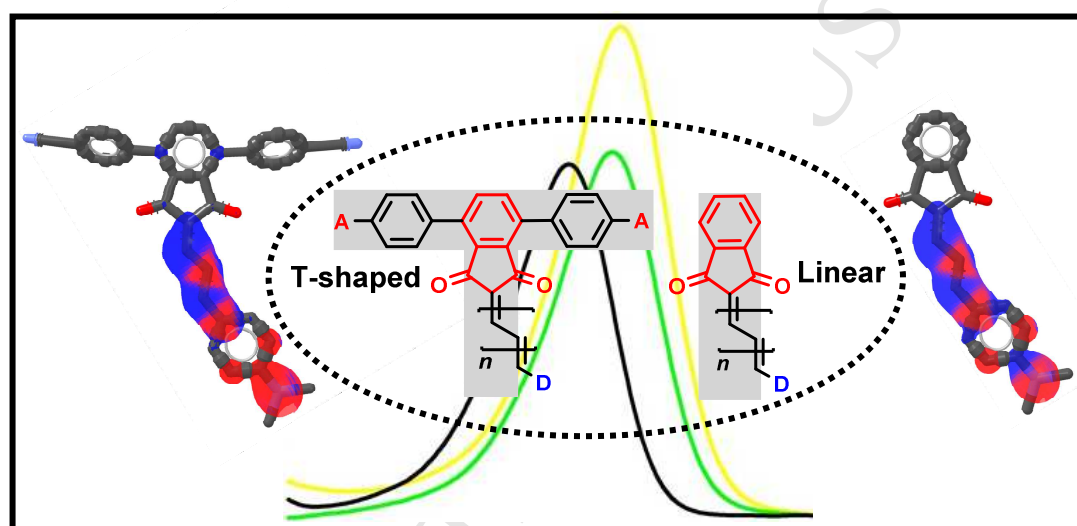
Abstract

A series of tripodal push-pull chromophores based on central indan-1,3-dione scaffold

has been designed and synthesized by Knoevenagel condensation and Pd-catalyzed

Suzuki-Miyaura cross-coupling reaction. Target molecules possess D−π−A−(π−A)₂

extraordinary T-shaped structural arrangement. The electron donor attached at $C2$

position as well as the peripheral acceptor branches at $C4$ and $C7$ positions of the

parent indan-1,3-dione have been systematically modified to achieve property tuning.

Fundamental thermal and optoelectronic properties have been investigated by

differential scanning calorimetry, electrochemistry, UV/Vis absorption spectroscopy,

and DFT calculations. Based on the experimental and theoretical data, we herewith discuss thorough structure–property relationships.

Keywords: indan-1,3-dione; T-shaped; donor/acceptor; intramolecular charge-transfer; push-pull chromophore.

Introduction

During the last 30–40 years, a great progress in developing new push-pull systems has been performed. Push-pull chromophores have become very popular and important substances used across many areas of materials chemistry. Nowadays, they represent well-developed and burgeoning area especially targeting organic electronics and optoelectronics.[1-2] Wide applications of push-pull molecules can be attributed to their unique features such as their well-defined and tunable structural arrangement.[3] The optoelectronic properties such as color, high (hyper)polarizabilities, intensive absorption, emission, and electrochemical behavior are predominantly controlled by the extent of the intramolecular charge-transfer (ICT), which is dictated by a mutual communication between the particular donor (D) and acceptor (A) *via* a π-linker.[4-7] Hence, push-pull chromophores have been utilized as active materials in nonliear optics,[8-10] bulk heterojunction (BHJs)[11-13] or dye sensitized solar cells (DSSCs),[14-16] organic light-emitting diodes (OLEDs),[17] organic field-effect transistors (OFETs),[18-20] two-photon absorbers (2PAs),[21-22] 3D optical data storage,[23-25] etc.

With respect to its commercial availability, low cost, extended π-system, and strong electron accepting character, indan-1,3-dione and its derivatives are widely used as terminal withdrawing moieties in push-pull chromophores.[26] Incorporation of indan-1,3-dione fragment into the chromophore backbone can be accomplished very

conveniently via Knoevenagel condensation under mild reaction conditions.[27-34] These features predestinate push-pull systems with indan-1,3-dione acceptors to be applied in nonlinear optics,[35-46] DSSCs,[47] BHJSCs,[48-49] organic photovoltaic cells (OPVCs),[50-51] OLEDs,[52] as vesicle-, gel-, and glass-forming molecules[53-54] or chromoionophores for anion sensing and recognition.[55-57] Indan-1,3-dione-terminated push-pull molecules may adopt linear (D-π-A) or various extraordinary arrangements resembling letters of the alphabet.[58] Recently we focused our research efforts towards new class of T-shaped molecules that utilizes indan-1,3-dione as a central acceptor and π-conjugated backbone.[59-60] Thus, the indan-1,3-dione was modified not only at $C2$ position but also at positions $C4$ and $C7$ of the fused benzene ring to afford tripodal D–π–A–(π–D)$_2$ molecules applicable in BHJSCs.[61] More recently, we have investigated a series of linear, quadrupolar, and T-shaped chromophores with varied number of peripheral electron donors.[62]

In order to further elucidate the structure-property relationships in indan-1,3-dione based push-pull molecules and in contrast to previously published T-shaped molecules having (D–π–A–(π–D)$_2$,[62] we report herein nonsymmetrical T-shaped chromophores **1–2** with novel D–π–A–(π–A)$_2$ structural arrangement (Figure 1). Whereas the branch at $C2$ remained donor-substituted, two peripheral branches at $C4$ and $C7$ bear auxiliary acceptors. Both series differ in the peripheral acceptors A (CN vs NO$_2$; **1** vs. **2**), the donor D (DMA vs. PIT; **a/b** vs. **c/d**), and the number of double bonds within the $C2$ donor branch ($n = 0$ or 1; **a/c** vs. **b/d**). Previously reported linear D–π–A chromophores **3a–d** without peripheral $C4/C7$ substituents have also been included in the study to facilitate elucidation of the structure-property relationships.[26]
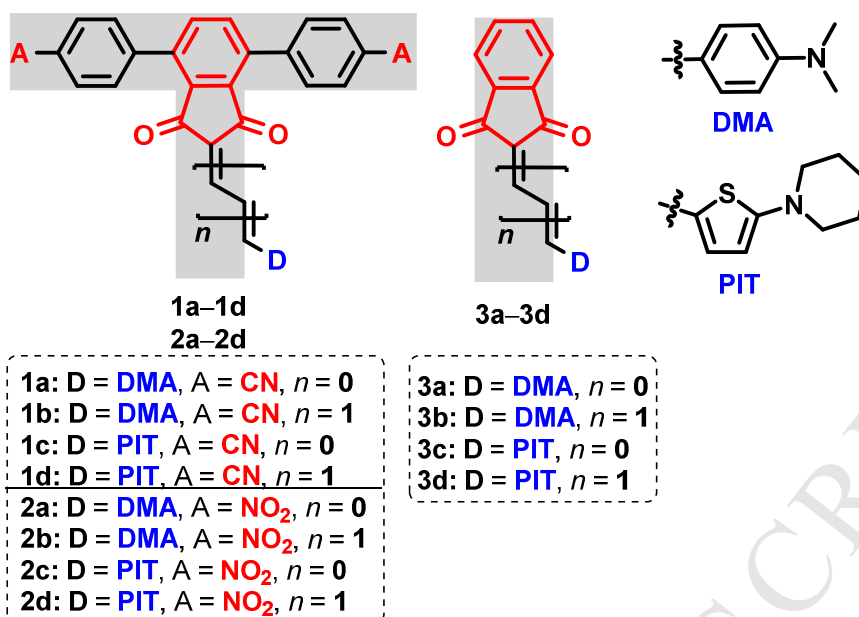
Figure 1: Structural arrangements of tripodal T-shaped and linear indan-1,3-dione chromophores **1–3**. DMA = 4-(*N,N*-dimethylamino)phenyl; PIT = 5-(piperidin-1-yl)thiophen-2-yl.

Results and Discussion

Synthesis

T-shaped chromophores **1** and **2** were prepared by Pd-catalyzed Suzuki-Miyaura cross-coupling reactions (Scheme 1) between boronic acids **5** and **6** and particular 4,7-diiodoindan-1,3-dione derivatives **4a–d** under standard reaction conditions in satisfactory yields (52–76 %). Linear chromophores **3a-b** were synthesized via Al$_2$O$_3$-catalyzed Knoevenagel condensation starting from commercial available indan-1,3-dione **7** and benzaldehyde **8** or cinnamaldehyde **9** with the yields about 80 %. The preparations and full characterization of remaining linear molecules **3c–d** as well as indan-1,3-dione intermediates **4a–d** were described in our recent reports.[26,59-60]
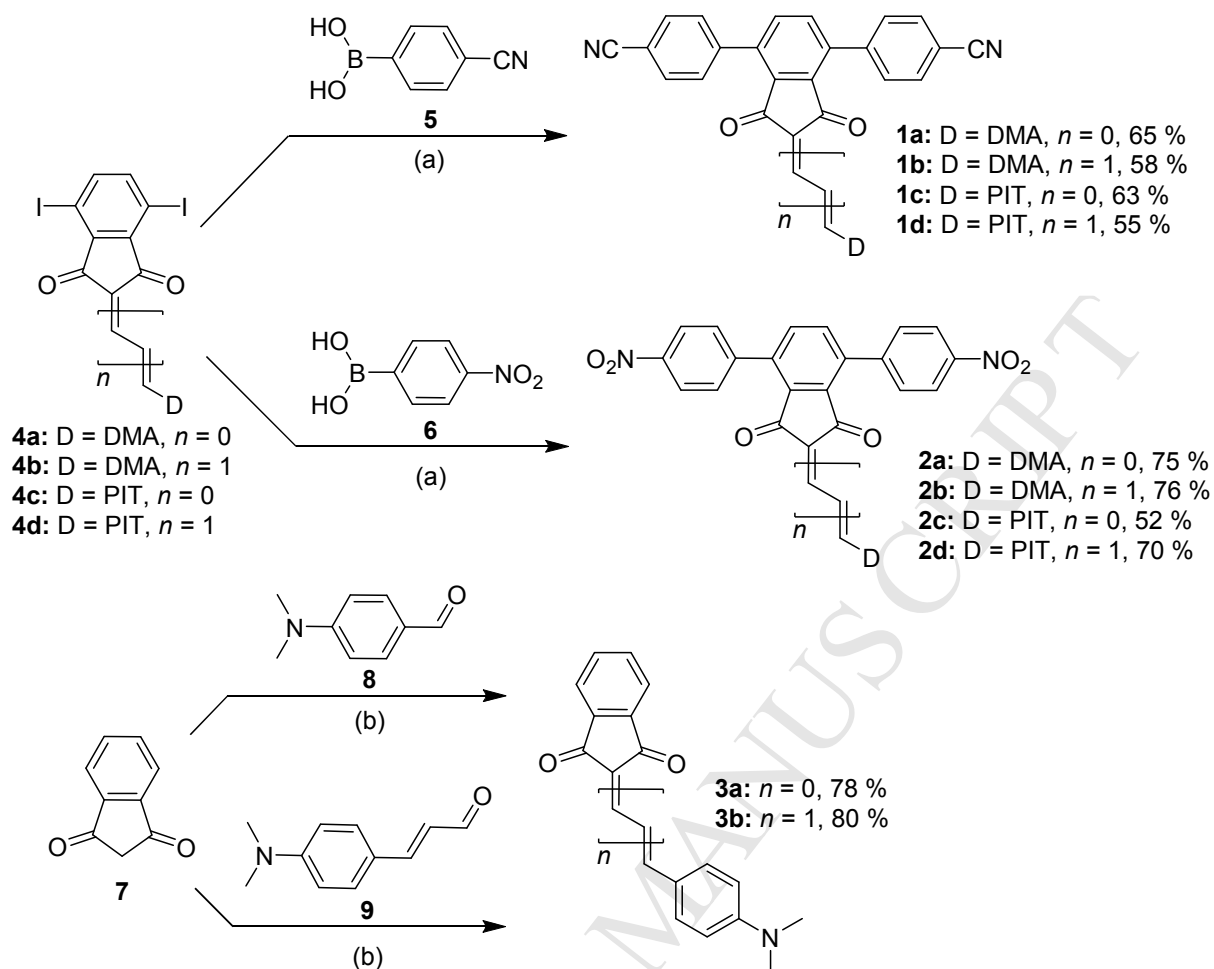
Scheme 1: Synthetic pathway towards linear and T-shaped indan-1,3-dione based chromophores **1–3**. (a) THF/H$_2$O 4:1, PdCl$_2$(PPh$_3$)$_2$, Na$_2$CO$_3$; (b) CH$_2$Cl$_2$, Al$_2$O$_3$ (activity II–III).

Thermal properties

Thermal characteristics of target chromophores **1-3** were measured by differential scanning calorimetry. The DSC curves were determined with a scanning rate of 3 °C/min within the range 25–400 °C. The measured melting points (T_m) as well as the decomposition temperatures (T_d) are summarized in Table 1. Representative DSC curves are shown in Figure 2, for all DSC curves see the SI.

T-shaped molecules **1** with peripheral cyano acceptors showed melting (Figure 2) immediately followed by exothermal and very vigorous decomposition (**1b**, **1c**) or the melting process is directly accompanied by degradation (**1a, 1d**). Thermal behavior of the nitro derivatives **2a−d** is dominated by direct decomposition without previous melting. Linear D−π−A analogues **3b−3d** with extended π-system underwent sharp melting process accompanied by gradual degradation. On the contrary, linear molecules **3a**/**3c** proved to be stable in the liquid phase for additional 70 °C after their melting.
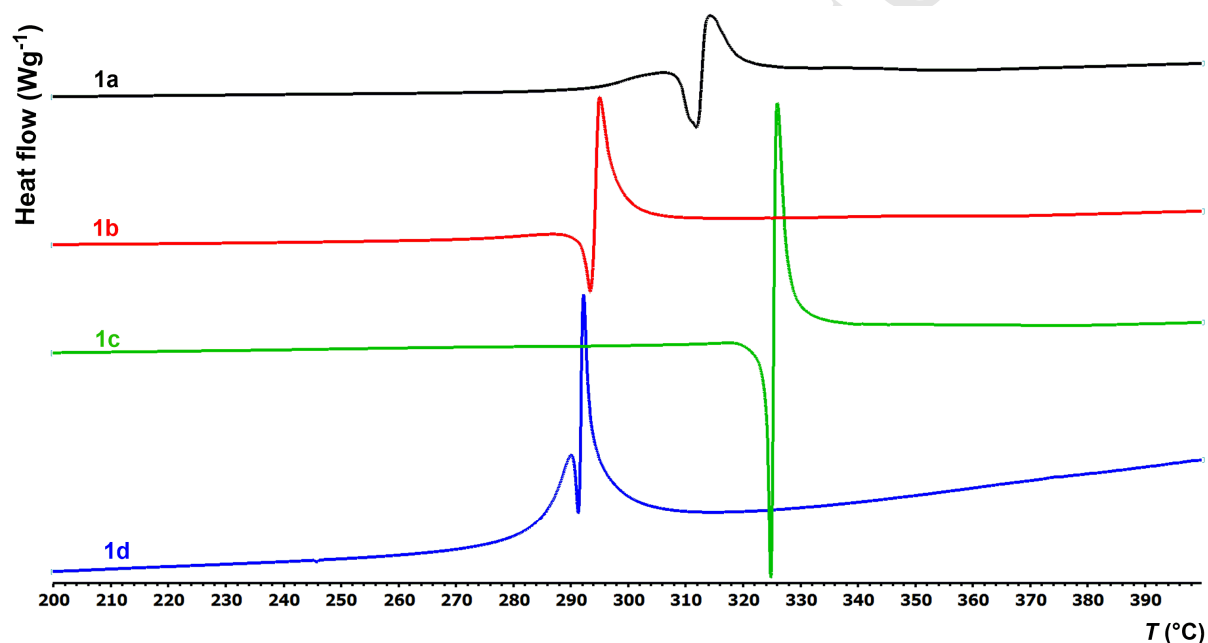
Figure 2: Representative DSC curves for chromophores **1a−d** with peripheral cyano acceptors within the range of 200−400 °C (melting and decomposition peaks are visualized).

In general, all studied compounds are highly thermally robust, especially T-shaped ones with the temperature of decomposition ranging from 240 to 330 °C. Linear chromophores **3a−b** bearing DMA donor provided higher T_m and T_d values, compared to PIT analogues **3c−d**. From the DSC data is also obvious that embedding

the double bond ($n = 0$ or 1) led to increased T_m and T_d values for all molecules under the study. In contrast to linear series **3**, the highest T_d values in T-shaped series **1–2** have been detected for molecules **1c/2c** ($T_d = 327/330$ °C) with appended PIT donor. Cyano (**1**) as well as nitro derivatives (**2**) afforded comparable temperatures of decomposition. Thus, the type of the peripheral acceptor group influences thermal stability of T-shaped indan-1,3-diones only negligibly.

Table 1: Thermal, electrochemical, and absorption properties of chromophores **1–3**.

Comp.	T_m [°C][a]	T_d [°C][b]	$E_{p(ox1)}$ [V][c]	$E_{p(red1)}$ [V][c]	ΔE [eV][c]	E_{HOMO} [eV][d]	E_{LUMO} [eV][d]	λ_{max}^{A} [nm/eV][e]	ε_{max} [10^3 M^{-1}cm^{-1}][e]
1a	-	295	1.04	−1.11	2.15	−5.43	−3.28	501/2.48	46.9
1b	292	295	0.86	−0.90	1.76	−5.25	−3.49	566/2.19	43.4
1c	324	327	0.83	−1.16	1.99	−5.22	−3.23	532/2.33	80.0
1d	-	284	0.61	−0.90	1.51	−5.00	−3.49	630/1.97	68.3
2a	-	299	1.07	−1.02	2.09	−5.46	−3.37	504/2.46	62.9
2b	-	243	0.88	−0.88	1.76	−5.27	−3.51	569/2.18	41.3
2c	-	330	0.84	−1.11	1.95	−5.23	−3.28	534/2.32	81.6
2d	-	272	0.61	−0.89	1.50	−5.00	−3.50	634/1.96	83.5
3a	203	274	1.05	−1.20	2.25	−5.44	−3.19	483/2.57	45.3
3b	253	257	0.84	−0.95	1.79	−5.23	−3.44	535/2.32	42.9
3c	182	246	0.80	−1.23	2.03	−5.19	−3.16	516/2.40	90.6
3d	208	213	0.57	−0.94	1.51	-4.96	−3.45	605/2.05	71.4

[a]T_m = melting point (the point of intersection of a baseline and a tangent of thermal effect = onset). [b]T_d = thermal decomposition (pyrolysis in N$_2$ atmosphere). [c]$E_{p(ox1)}$ and $E_{p(red1)}$ are peak potentials of the first oxidation and reduction (irreversible processes), respectively, as measured by CV; all potentials are given *vs.* SSCE, $\Delta E = E_{p(ox1)} - E_{p(red1)}$. [d] $-E_{HOMO/LUMO} = E_{p(ox1/red1)} + 4.35$ (in DMF vs. SCE)[63] $+ 0.036$ (difference between SCE (0.241 vs. SHE) and SSCE (0.205 vs. SHE))[64]. [e]Measured in CH$_2$Cl$_2$.

Electrochemistry

The electrochemical behavior of target chromophores **1**–**3** were investigated by cyclic voltammetry in DMF containing 0.1 M Bu_4NBF_4 in a three electrode cell by cyclic voltammetry (CV). The working electrode was glassy carbon disk (1 mm in diameter). As the reference and auxiliary electrodes were used leakless Ag/AgCl electrode (SSCE) containing filling electrolyte (3.4 M KCl) and titanium rod with a thick coating of platinum, respectively. All peak potentials are given *vs*. SSCE. The acquired data are summarized in Table 1; representative CV diagrams of compounds **1d**, **2d**, and **3d** are given in the SI.

The observed first oxidations and reductions were determined as irreversible processes (quasi-reversible for some molecules) generally followed by subsequent oxidations and reductions. Therefore, the potentials of the first oxidation and reduction were obtained only as peak potentials $E_{p(ox1/red1)}$ which were found within the range of 0.57 to 1.07 and -1.23 to -0.88 V, respectively. The first oxidation and reduction are typical one-electron processes; their potentials are obviously a function of the chromophore structure. Whereas the first oxidation takes place predominantly at the amino donor group, the first reduction most likely involves the central indan-1,3-dione as well as the *C*4 and *C*7 peripheral acceptors. The peak potentials of the first oxidation and reduction were further recalculated to the energies of the HOMO and the LUMO (Table 1) and these values were visualized in the energy level diagram (Figure 3). Despite the fact that the electrochemically derived peak potentials do not correspond in absolute values with the HOMO/LUMO levels (half-wave potentials not available), these values can be used for describing the trends within the given series of molecules.
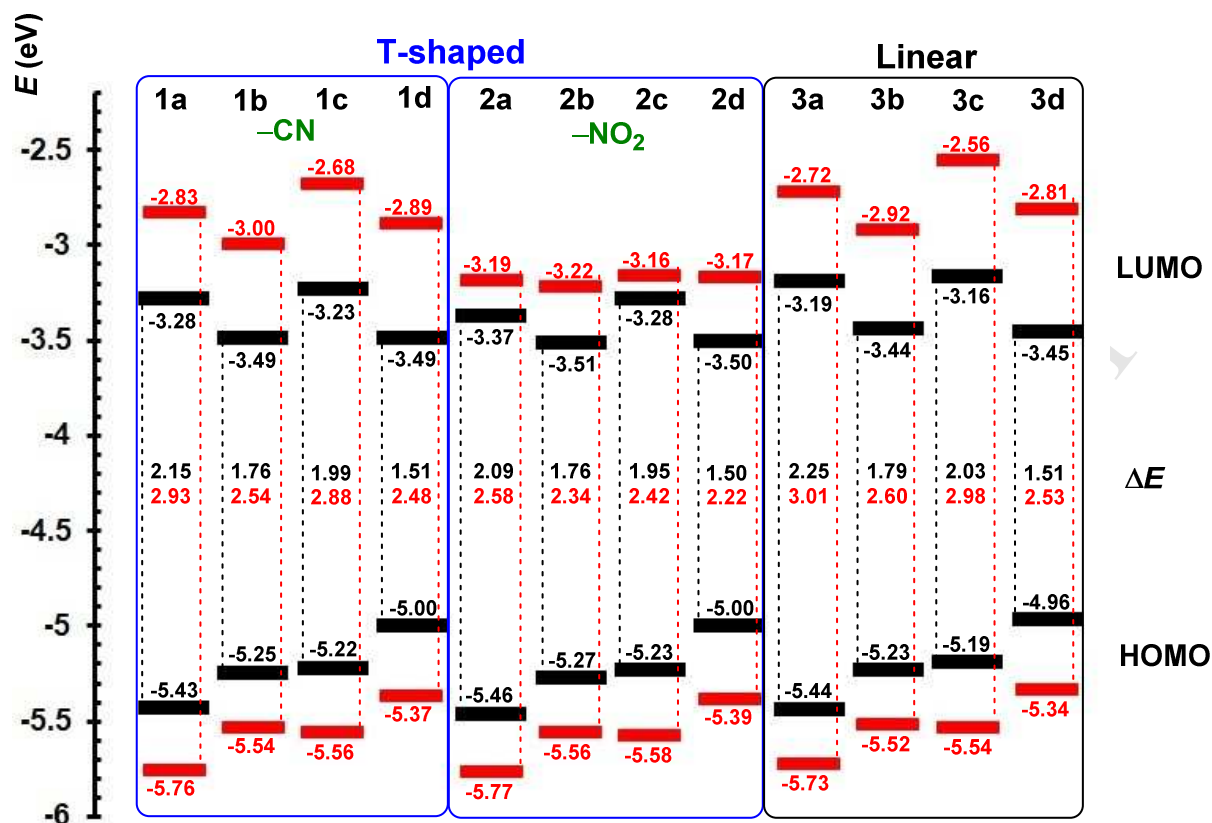
Figure 3: Energy level diagram of electrochemical (black) and DFT calculated (red) HOMO/LUMO energies of chromophores **1–3**.

A comparison of the electrochemical data allows to deduce the following general trends and relationships:

- The HOMO levels reflect solely the used donor D (DMA *vs.* PIT) as well as the length of the $C2$-appended π-linker ($n = 0$ or 1) and is almost not influenced by the presence of peripheral acceptors A. For analogous chromophores (e.g. **1b/2b/3b**) are the HOMO energies very close (−5.25/−5.27/−5.23 eV). The E_{HOMO} values gradually increase within the order: **a** (DMA) → **b** (DMA + =) → **c** (PIT) → **d** (PIT + =); see Table 1 and Figure 3 (= stands for an additional double bond).

- The LUMO level is affected by the peripheral acceptors A and less by the donor and the length of the π-linker. As expected, the LUMO values decrease

within the order: **3** → **1** → **2** (e.g. −3.16/−3.23/−3.28 eV for **3c/1c/2c**). This reflects none auxiliary acceptors (**3**) and higher electron withdrawing ability of the nitro (**2**) over the CN (**3**) group.[3] π-Linker enlargement generally deepened the measured E_{LUMO} values (compare **a** vs. **b** or **c** vs. **d** series of molecules). In overall, the LUMO levels alternate within the order: ↑**a** ↓**b** ↑**c** ↓**d**; see Table 1 and Figure 3.

- The HOMO-LUMO gap (Δ*E*) is predominantly influenced by the length of π-backbone as well as the type of the used donor. The spatial arrangement of chromophore (linear *vs*. T-shaped) affects the electrochemical gap rather less substantially. Considering the particular chromophore parts, the HOMO-LUMO gap decreases within the order: **3** (none auxiliary acceptor) → **1** (−CN) → **2** (−NO$_2$), e.g. 2.25/2.15/2.09 eV for **3a/1a/2a**; **a** (DMA) → **c** (PIT) → **b** (DMA + =) → **d** (PIT + =), e.g. 2.15/1.99/1.76/1.51 eV for **1a/1c/1b/1d**; see Table 1, Figure 3.

In summary, the HOMO/LUMO levels are affected by the type and the length of donor branch attached at *C*2-position. Utilization of polarizable PIT donor and extension of *C*2-backbone via additional ethylene spacer lead to significant reduction of Δ*E*. On the contrary, introducing auxiliary peripheral acceptors at *C*4 and *C*7 improves the overall withdrawing ability only negligibly. As expected, the nitro group proved to be slightly more powerful acceptor than cyano. Hence, the lowest electrochemical HOMO-LUMO gap was determined for T-shaped indan-1,3-dione chromophore **2d** (Δ*E* = 1.50 eV) possessing PIT donor attached at the extended π-linker and two peripheral 4-nitrophenyl withdrawing units.
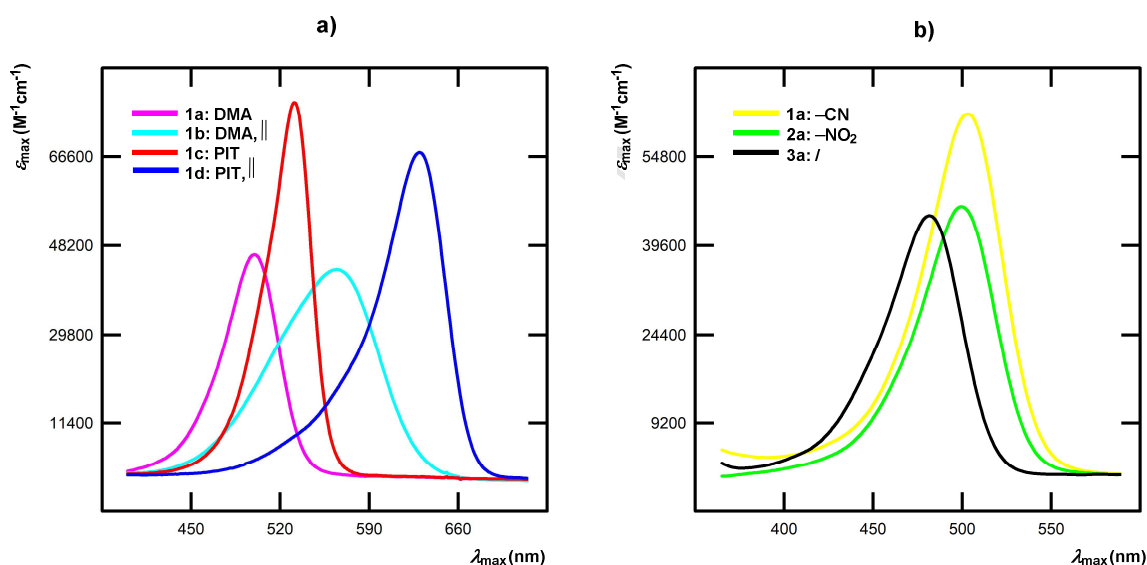
Electronic absorption spectra

Chromophores **1–3** represent highly colored substances with the color ranging from dark red to blue; their linear optical properties were investigated by UV-Vis absorption spectroscopy. Fluorescence behavior was not observed and, therefore, emission spectra were not measured. The measured longest-wavelength absorption maxima λ_{max} and molar extinction coefficients ε_{max} are summarized in Table 1. The λ_{max} values range from 483 to 634 nm with the ε_{max} found within the range of $41.3–90.6 \times 10^3 \, M^{-1} \cdot cm^{-1}$. Representative absorption spectra of chromophores **1a–d** with peripheral cyano acceptors as well as a series of compounds **1a**, **2a**, and **3a** with $C2$-attached DMA donor branch are shown in Figure 4. For complete listing see the SI. The absorption spectra of chromophores **1–3** exhibited one apparent CT-band, its position correlates tightly with the electrochemical gaps as shown in the SI (Figure S35).

From the measured data we can deduce the following trends:

- Positions of the CT-bands are influenced by the type of the peripheral withdrawing unit only negligibly. The difference ($\Delta\lambda_{max}$) between cyano (**1a–d**) and nitro (**2a–d**) analogues is only 2–4 nm; see Table 1 or Figure 4b.

- The absence of auxiliary peripheral acceptors blue-shifts the CT-bands by about 15–35 nm; compare series **3** vs. **1–2** in Figure 4b.

- The presence of polarizable PIT donor in series **c–d** clearly red-shifts the CT-bands compared to DMA donor in series **a–b**. This red-shift is considerably pronounced for molecules with embedded double bond; **b** vs. **d** in Figure 4a.

- Chromophores in series **c–d** bearing PIT donor showed considerably higher molar extinction coefficients (Figure 4a).

- Embedding an additional double bond into the π-linker causes distinct bathochromic shift of about 50−65/90−100 nm for chromophores with attached DMA/PIT donors; compare compounds **1b**/**1d** vs. **1a**/**1c** in Figure 4a.

The optical properties of chromophores **1**−**3** are predominantly dictated by (in descending order): the type of *C*2 donor used, the extent of π-linker, and the structural/spatial arrangement (linear vs. T-shaped; presence of the auxiliary acceptors). Hence, the most bathochromically shifted CT-band (634 nm) has been observed for T-shaped push-pull chromophore **2d** that possesses two auxiliary peripheral nitro acceptors, extended π-linker, and polarizable PIT donor. This correspond to electrochemical outcomes.

Figure 4: a) Representative UV/Vis absorption spectra of chromophores **1a**–**d** bearing peripheral cyano acceptors; b) representative absorption spectra of chromophores **1a**, **2a**, and **3a** with attached DMA donor at *C*2-position (measured in CH_2Cl_2 at $c \approx 2 \times 10^{-5}$ M).

Theoretical DFT calculations

Spatial and electronic properties of linear and T-shaped chromophores **1–3** were investigated using Gaussian$^{(R)}$ 16 software package[65] at the DFT level. Initial geometries of molecules **1–3** were optimized by DFT B3LYP/6-311+G(2d,p) method. Energies of the HOMO and the LUMO, their differences ΔE and ground state dipole moments μ were calculated at DFT B3LYP/6-311+G(2d,p) level in vacuum, acetonitrile (AN), and DMF. The first hyperpolarizabilities β were computed at DFT B3LYP/6-311+G(2d,p) level in CH_2Cl_2 at 1907 nm. All calculated data are summarized in Table 2.

The calculated HOMO/LUMO energies in both solvents proved to be identical due to very similar parameters of both solvents in the PCM solvation model (ε_{AN} = 35.7; ε_{DMF} = 37.2). The HOMO/LUMO energies in vacuum are listed in Table S1. The relationships between the HOMO/LUMO energies calculated for vacuum and polar solvent are depicted in Figures S36–S37. The plotted points are in these graphs divided by a line featuring unit slope and zero intercept, which clearly distinguishes (de)stabilization induced by the solvent. Figure S36 shows that, in contrast to linear molecules **3**, the HOMOs of T-shaped chromophores **1–2** are stabilized by polar solvent (an apparent collinearity with the line). The LUMOs are stabilized only for cyano derivatives **1**, which E_{LUMO} is collinear and localized above the line (Figure S37). Linear chromophores **3** and T-shaped nitro derivatives **2** showed E_{LUMO} localized below the line, either collinear or as a cluster of points.

The calculated HOMO and LUMO energies range from −5.77 to −5.34 and −3.22 to −2.56 eV and showed dependence on the structural arrangement of the particular chromophore. The HOMO energies correlate very tightly with the

experimental data obtained by the electrochemical measurements as shown in Figure S38. On the contrary, the withdrawing ability of peripheral nitro acceptors in T-shaped molecules **2** is computationally overestimated. Hence, the calculated LUMO levels for nitro derivatives **2a–d** are the lowest, almost identical (−3.16 to −3.22 eV), and not reflecting the alternating trend as seen by electrochemistry for the remaining chromophores **1a–d** and **3a–d** (Figure 3). This phenomenon is clearly depicted in Figure S39 showing the LUMO energies of T-shaped nitro derivatives **2** distinctly separated from the others. This overestimation also influences the calculated gaps of T-shaped nitro derivatives **2**, which are obviously narrowed compared to linear **3** as well as T-shaped **1** (Figure 3). The calculated HOMO/LUMO energies and their differences are affected by the same structural modifications and keep the same trends as seen by electrochemical measurements. The length of the π-linker attached at *C*2 position proved the most crucial factor, whereas type of the donor (DMA vs. PIT) and the auxiliary acceptor affected the calculated properties less obviously. A similar set of calculated $E_{HOMO/LUMO}$ and ΔE values for T-shaped **1** and linear **3** (Table 2) also points to a poor involvement of auxiliary acceptors in the ICT.

The frontier molecular orbital's localizations in representative chromophores **1b**, **2b**, and **3b** are shown in Figure 5; for complete listing see the SI. As a general feature, the HOMO-1 is localized on the DMA and PIT donor, respectively, whereas the LUMO+1 is spread over the central withdrawing indan-1,3-dione moiety. The HOMO is localized on the *C*2 donor-substituted branch jointly with the LUMO and a partial separation. In T-shaped molecules **1**–**2**, the LUMO may further occupy the indan-1,3-dione fused ring as well as the peripheral phenylene rings.
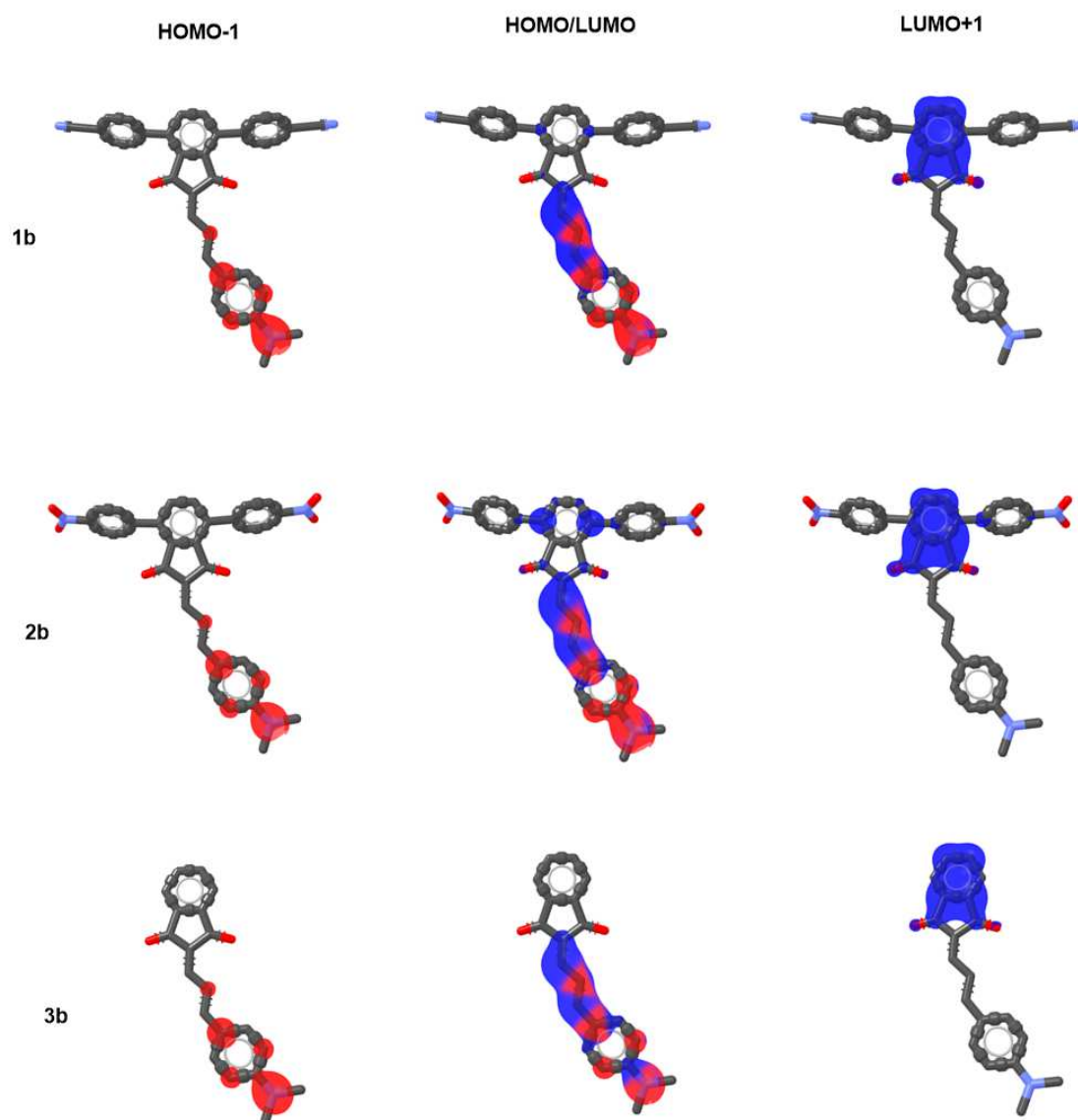
Figure 5: The HOMO (red) an LUMO (blue) localizations in representative chromophores **1b**, **2b**, and **3b**.

Whereas linear chromophores **3a–b** with DMA donor possess *C*s group of symmetry, the remaining target molecules are non-symmetrical. There is an apparent trend in ground state dipole moments μ for molecules **1–3** (Table 2). The dipole moments obey the trend seen for the HOMO energies (Figure S40). The lowest/highest μ values were calculated for chromophores in series **a**/**d** possessing elementary DMA/extended PIT donor, whereas the **b**/**c** pairs provided comparable

μ values. Linear chromophores **3** afforded generally lower dipole moments compared to T-shaped analogous **1–2** (e.g. 16.9 → 18.7 → 19.2 D for **3d**/**1d**/**2d**).

Table 2: DFT calculated properties of chromophores **1–3**.

Comp.	E_{HOMO} [eV][a]	E_{LUMO} [eV][a]	ΔE [eV][a]	μ [D][a]	$\beta \times 10^{-30}$ [esu][b]
1a	−5.76	−2.83	2.93	10.3	155
1b	−5.54	−3.00	2.54	13.9	401
1c	−5.56	−2.68	2.88	13.8	95
1d	−5.37	−2.89	2.48	18.7	234
2a	−5.77	−3.19	2.58	10.6	195
2b	−5.56	−3.22	2.34	14.3	486
2c	−5.58	−3.16	2.42	14.1	154
2d	−5.39	−3.17	2.22	19.2	355
3a	−5.73	−2.72	3.01	8.5	108
3b	−5.52	−2.92	2.60	11.9	312
3c	−5.54	−2.56	2.98	12.1	57
3d	−5.34	−2.81	2.53	16.9	158

[a] Calculated at the DFT B3LYP/6-311+G(2d,p) level in DMF/AN. [b] Calculated at the DFT B3LYP/6-311+G(2d,p) level in CH_2Cl_2 at 1907 nm (−2ω;ω,ω).

The calculated first hyperpolarizabilities β range from 57 to 486 × 10^{-30} esu for linear as well as T-shaped compounds **1–3**, respectively (Table 2). In general, clear trend in increasing β values with the π-linker elongation/planarization was observed (e.g. 155/401 × 10^{-30} esu for **1a**/**1b**). The type of $C2$ donor plays also a crucial role. The larger first hyperpolarizabilities were computed for chromophores bearing DMA donor compared to the corresponding PIT derivative (e.g. 155/95 × 10^{-30} esu for

1a/**1c**). Concerning the spatial arrangement, the β values increase within the order: linear **3** → T-shaped **1** (cyano) → T-shaped **2** (nitro). Based on the aforementioned trends, the largest first hyperpolarizability $\beta = 486 \times 10^{-30}$ esu was calculated for T-shaped chromophore **2b** possessing extended DMA donor branch and peripheral auxiliary nitro acceptors.

Conclusion

As a continuation and further extension of our previous studies on linear D-π-A, quadrupolar (D-π)$_2$-A, and tripodal (D-π)$_3$-A push-pull chromophores built on central electron-withdrawing indan-1,3-dione moiety, [59-62] we have reported herein the new strategy to design molecules with D-π-A-(π-A)$_2$ structural arrangement. In overall, eight new push-pull chromophores **1a–d** and **2a–d** with tripodal T-shaped arrangement have been prepared together with four linear analogues **3a–d**. *N*,*N*-Dimethylanilino and 2-(piperidin-1-yl)thiophen with systematically enlarged π-linker via embedded double bond have been utilized as electron donors attached to the central indan-1,3-dione at *C*2 position via Knoevenagel condensation. Peripheral 4-cyanophenyl and 4-nitrophenyl acceptors were introduced at *C*4/*C*7 via subsequent Pd-catalyzed twofold Suzuki-Miyaura cross-coupling reaction.

Thermal properties studied by DSC revealed thermal robustness of all T-shaped molecules with T_d between 213 and 330 °C. The extent of the ICT has been evaluated by electrochemical measurements and UV/Vis absorption spectra and completed by DFT calculations. From the gathered data we can conclude that the fundamental property tuning in chromophores **1–3** can be achieved by alternating the type of electron donor appended at *C*2 (DMA vs. PIT) and the π-backbone length. The

presence of auxiliary acceptors at *C*4/*C*7 positions has diminished effect and can rather be used for final fine-tuning.

As mentioned earlier, indan-1,3-dione push-pull molecules found tremendous applications across nonlinear optics, organic-based solar and photovoltaic cells or as sensors for ion recognition. In view of the current interest in organic push-pull molecules with various arrangement and tunable properties, the present study is intended to serve as an useful guide for the advanced design of functional indan-1,3-dione derivatives.

Experimental section

General

All target T-shaped chromophores **1a**–**d** and **2a**–**d** are new compounds. Linear compounds **3c**–**d** with PIT donor were firstly prepared in our recent study.[26] The linear chromophore **3a** is well known.[66] Full structural characterization such as ^{13}C-NMR or HR-MS analyses are not available for remaining linear molecule **3b**.[67] Details concerning material, apparatus, and methods are provided in the SI. Synthesis and full spectral characterization of previously known target chromophores **3a–b** is given in the SI.

General Method for Suzuki-Miyaura Cross-couplig Reaction (i)

4,7-Diiodoindan-1,3-dione **4a**, **4b**, **4c** or **4d** (265, 278, 288, 300 mg; 0.5 mmol) and 4-cyanophenylboronic acid **5** (162 mg, 1.1 mmol) or 4-nitrophenylboronic acid (187 mg, 1.1 mmol) were dissolved in the mixture of THF/H_2O (20 mL, 4:1). Argon was bubbled through the solution for 15 min whereupon [$PdCl_2(PPh_3)_2$] (18 mg, 0.025 mmol) and Na_2CO_3 (159 mg, 1.5 mmol) were added and the reaction mixture was stirred at 60 °C for 3 h. The reaction was diluted with H_2O (50 mL) and extracted with

CH$_2$Cl$_2$ (2 × 50 mL). The combined organic extracts were dried (Na$_2$SO$_4$), the solvents were evaporated *in vacuo*, and the crude product was purified by column chromatography.

General Method for Al$_2$O$_3$-Catalyzed Knoevenagel Condensation (ii)

Indan-1,3-dione **7** (1.46 g, 10.0 mmol) and 4-(*N,N*-dimethylamino)benzaldehyde **8** (1.57 g, 10.5 mmol) or 4-(*N,N*-dimethylamino)cinnamaldehyde **9** (1.84 g, 10.5 mmol) were dissolved in CH$_2$Cl$_2$ (20 mL), Al$_2$O$_3$ (5.1 g, 50.0 mmol, activity II-III) was added and the reaction mixture was stirred at 25 °C for 3 h. Al$_2$O$_3$ was filtered off, the solvent was evaporated *in vacuo*, and the crude product was purified by column chromatography.

Chromophore 1a. The title compound was prepared from 4,7-diiodoindan-1,3-dione **4a** and boronic acid **5** following the general procedure (i). The title compound was afforded as a red solid (156 mg, 65 %). R_f = 0.25 (SiO$_2$; CH$_2$Cl$_2$/hexane, 3:1). ^{1}H-NMR (400 MHz, CDCl$_3$, 25 °C): δ = 3.13 (s, 6H, CH$_3$), 6.68 (d, J = 8.8 Hz, 2H, CH$_{ar}$), 7.55–7.60 (m, 2H, CH$_{ar}$), 7.64–7.68 (m, 5H, CH+CH$_{ar}$), 7.76–7.79 (m, 4H, CH$_{ar}$), 8.40 ppm (d, J = 8.4 Hz, 2H, CH$_{ar}$). ^{13}C-NMR (125 MHz, CDCl$_3$, 25 °C): δ = 40.37, 111.73, 112.14, 112.20, 119.11, 119.18, 121.92, 122.11, 130.46, 130.49, 131.86, 131.92, 135.54, 136.13, 136.70, 138.30, 138.38, 138.79, 142.45, 142.92, 148.74, 154.56, 188.58, 190.40 ppm. HR-MALDI-MS (DHB): calcd for C$_{32}$H$_{22}$N$_3$O$_2$ (M+H)$^+$ 480.17065; found 480.17067. IR (HATR): ν = 2913, 2224, 1664, 1557, 1515, 1377, 1324, 1177, 1114, 814, 525 cm^{-1}.

Chromophore 1b. The title compound was prepared from 4,7-diiodoindan-1,3-dione **4b** and boronic acid **5** following the general procedure (i). The title compound was afforded as a brown-black solid (158 mg, 58 %). R_f = 0.20 (SiO$_2$; CH$_2$Cl$_2$/hexane, 3:1).

^{1}H-NMR (400 MHz, CDCl$_3$, 25 °C): δ = 3.08 (s, 6H, CH$_3$), 6.67 (d, J = 8.8 Hz, 2H, CH$_{ar}$), 7.28 (d, J = 15.2 Hz, 1H, CH), 7.53–7.61 (m, 5H, CH+CH$_{ar}$), 7.63–7.66 (m, 4H, CH$_{ar}$), 7.75–7.80 (m, 4H, CH$_{ar}$), 8.14 ppm (dd, J_1 = 15.2 Hz, J_2 = 12.4 Hz, 1H, CH). ^{13}C-NMR (125 MHz, CDCl$_3$, 25 °C): δ = 40.40, 112.10, 112.27, 112.31, 119.10, 119.40, 123.06, 123.74, 130.40, 130.46, 131.89, 131.94, 132.17, 135.80, 136.01, 137.40, 138.29, 138.49, 138.64, 142.27, 142.61, 148.07, 153.06, 155.83, 189.41, 189.95 ppm. HR-MALDI-MS (DHB): calcd for C$_{34}$H$_{24}$N$_3$O$_2$ (M+H)$^+$ 506.18630; found 506.18573. IR (HATR): ν = 2921, 2225, 1669, 1556, 1380, 1325, 1174, 813, 547 cm^{-1}.

Chromophore 1c. The title compound was prepared from 4,7-diiodoindan-1,3-dione **4c** and boronic acid **5** following the general procedure (i). The title compound was afforded as a red-brown solid (165 mg, 63 %). R_f = 0.20 (SiO$_2$; CH$_2$Cl$_2$). ^{1}H-NMR (400 MHz, CDCl$_3$, 25 °C): δ = 1.72 (bs, 6H, CH$_2$), 3.53–3.54 (m, 4H, NCH$_2$), 6.26 (d, J = 4.0 Hz, 1H, CH$_{th}$), 7.47–7.60 (m, 4H, CH+CH$_{th}$+CH$_{ar}$), 7.67 (bs, 4H, CH$_{ar}$), 7.74–7.75 ppm (m, 4H, CH$_{ar}$). ^{13}C-NMR (125 MHz, CDCl$_3$, 25 °C): δ = 23.67, 25.51, 51.66, 108.34, 111.68, 111.79, 119.22, 119.33, 122.99, 130.53, 131.65, 131.83, 134.78, 135.28, 136.78, 136.99, 137.27, 137.99, 142.81, 143.05, 150.42, 173.70, 189.06, 190.05 ppm. HR-MALDI-MS (DHB): calcd for C$_{33}$H$_{24}$N$_3$O$_2$S (M+H)$^+$ 526.15837; found 526.15867. IR (HATR): ν = 2937, 2222, 1644, 1569, 1518, 1475, 1408, 1375, 1239, 1173, 1125, 1075, 1001, 823, 771, 558 cm^{-1}.

Chromophore 1d. The title compound was prepared from 4,7-diiodoindan-1,3-dione **4d** and boronic acid **5** following the general procedure (i). The title compound was afforded as a black solid (151 mg, 55 %). R_f = 0.20 (SiO$_2$; CH$_2$Cl$_2$). ^{1}H-NMR (500 MHz, CDCl$_3$, 25 °C): δ = 1.61 (bs, 2H, CH$_2$), 1.69–1.73 (m, 4H, CH$_2$), 3.41–3.43 (m, 4H, NCH$_2$), 6.10 (d, J = 4.5 Hz, 1H, CH$_{th}$), 7.22 (d, J = 4.5 Hz, 1H, CH$_{th}$), 7.33 (d, J =

14.0 Hz, 1H, CH), 7.41 (d, J = 12.5 Hz, 1H, CH), 7.50–7.51 (m, 2H, CH_{ar}), 7.60 (d, J = 13.5 Hz, 1H, CH), 7.65–7.66 (m, 4H, CH_{ar}), 7.74–7.78 ppm (m, 4H, CH_{ar}). ^{13}C-NMR (125 MHz, CDCl$_3$, 25 °C): δ = 23.70, 25.27, 51.72, 106.90, 111.98, 117.12, 119.22, 119.75, 126.11, 130.49, 131.76, 131.81, 135.12, 135.41, 137.26, 137.56, 137.82, 138.53, 140.82, 142.66, 143.04, 146.94, 147.86, 168.28, 189.69, 190.10 ppm. HR-MALDI-MS (DHB): calcd for $C_{35}H_{26}N_3O_2S$ (M+H)$^+$ 552.17402; found 552.17458. IR (HATR): ν = 2928, 2224, 1648, 1554, 1518, 1414, 1330, 1213, 1158, 1109, 1051, 987, 821 cm^{-1}.

Chromophore 2a. The title compound was prepared from 4,7-diiodoindan-1,3-dione **4a** and boronic acid **6** following the general procedure (i). The title compound was afforded as a red solid (195 mg, 75 %). R_f = 0.60 (SiO$_2$; CH$_2$Cl$_2$/hexane, 3:1). ^{1}H-NMR (400 MHz, CDCl$_3$, 25 °C): δ = 3.13 (s, 6H, CH$_3$), 6.68 (d, J = 9.2 Hz, 2H, CH_{ar}), 7.59–7.64 (m, 2H, CH_{ar}), 7.70–7.74 (m, 5H, CH+CH_{ar}), 8.33−8.41 ppm (m, 6H, CH_{ar}). ^{13}C-NMR (125 MHz, CDCl$_3$, 25 °C): δ = 40.37, 111.75, 121.82, 122.13, 123.34, 123.41, 130.66, 130.71, 135.48, 136.01, 136.81, 138.03, 138.13, 138.84, 138.93, 144.37, 144.88, 147.86, 147.92, 148.88, 154.61, 188.49, 190.31 ppm. HR-MALDI-MS (DHB): calcd for $C_{30}H_{22}N_3O_6$ (M+H)$^+$ 520.15032; found 520.15055. IR (HATR): ν = 2917, 1665, 1507, 1317, 1174, 1108, 1002, 828, 747, 694, 523 cm^{-1}.

Chromophore 2b. The title compound was prepared from 4,7-diiodoindan-1,3-dione **4b** and boronic acid **6** following the general procedure (i). The title compound was afforded as a black solid (207 mg, 76 %). R_f = 0.30 (SiO$_2$; CH$_2$Cl$_2$/hexane, 2:1). ^{1}H-NMR (400 MHz, CDCl$_3$, 25 °C): δ = 3.08 (s, 6H, CH$_3$), 6.67 (d, J = 8.8 Hz, 2H, CH_{ar}), 7.30 (d, J = 14.8 Hz, 1H, CH), 7.54–7.58 (m, 3H, CH+CH_{ar}), 7.61−7.65 (m, 2H, CH_{ar}), 7.71 (dd, J_1 = 8.4 Hz, J_2 = 2.8 Hz, 4H, CH_{ar}), 8.15 (dd, J_1 = 15.2 Hz, J_2 = 12.4 Hz, 1H, CH), 8.33–8.39 ppm (m, 4H, CH_{ar}). ^{13}C-NMR (125 MHz, CDCl$_3$, 25 °C): δ =

40.56, 112.36, 119.54, 123.04, 123.38, 123.44, 130.61, 130.68, 132.19, 135.77, 135.95, 137.50, 138.05, 138.24, 138.73, 144.17, 144.53, 147.93, 148.16, 152.88, 155.87, 189.33, 189.86 ppm. HR-MALDI-MS (DHB): calcd for $C_{32}H_{24}N_3O_6$ (M+H)$^+$ 546.16596; found 546.16667. IR (HATR): ν = 2920, 1665, 1552, 1507, 1343, 1323, 1171, 994, 817, 749, 696, 598 cm^{-1}.

Chromophore 2c. The title compound was prepared from 4,7-diiodoindan-1,3-dione **4c** and boronic acid **6** following the general procedure (i). The title compound was afforded as a red solid (159 mg, 52 %). R_f = 0.30 (SiO$_2$; CH$_2$Cl$_2$/hexane, 3:1). ^{1}H-NMR (500 MHz, CDCl$_3$, 25 °C): δ = 1.73 (bs, 6H, CH$_2$), 3.55 (bs, 4H, NCH$_2$), 6.27 (d, J = 4.5 Hz, 1H, CH$_{th}$), 7.52–7.62 (m, 4H, CH+CH$_{th}$+CH$_{ar}$), 7.73 (bs, 4H, CH$_{ar}$), 8.32–8.33 ppm (m, 4H, CH$_{ar}$). ^{13}C-NMR (125 MHz, CDCl$_3$, 25 °C): δ = 23.71, 25.56, 51.71, 108.47, 123.09, 123.20, 123.36, 130.76, 130.84, 134.75, 135.20, 136.93, 137.02, 137.10, 137.21, 138.15, 144.83, 145.07, 147.74, 150.61, 173.89, 190.03 ppm. HR-MALDI-MS (DHB): calcd for $C_{31}H_{24}N_3O_6S$ (M+H)$^+$ 566.13803; found 566.13867. IR (HATR): ν = 2931, 1651, 1569, 1510, 1332, 1240, 1181, 1130, 1072, 1003, 830, 747 cm^{-1}.

Chromophore 2d. The title compound was prepared from 4,7-diiodoindan-1,3-dione **4d** and boronic acid **6** following the general procedure (i). The title compound was afforded as a black solid (206 mg, 70 %). R_f = 0.25 (SiO$_2$; CH$_2$Cl$_2$/hexane, 3:1). ^{1}H-NMR (400 MHz, CDCl$_3$, 25 °C): δ = 1.57–1.70 (m, 6H, CH$_2$), 3.42 (bs, 4H, NCH$_2$), 6.10 (d, J = 4.0 Hz, 1H, CH$_{th}$), 7.23 (d, J = 4.5 Hz, 1H, CH$_{th}$), 7.34 (d, J = 14.0 Hz, 1H, CH), 7.43 (d, J = 12.4 Hz, 1H, CH), 7.54 (bs, 2H, CH$_{ar}$), 7.59–7.66 (m, 1H, CH), 7.71 (d, J = 7.6 Hz, 4H, CH$_{ar}$), 8.33 ppm (bs, 4H, CH$_{ar}$). ^{13}C-NMR (125 MHz, CDCl$_3$, 25 °C): δ = 23.68, 25.26, 51.73, 107.01, 117.11, 119.55, 123.24, 123.30, 126.14, 130.69, 135.02, 135.26, 137.26, 137.37, 137.53, 138.62, 141.03, 144.62, 144.99,

147.01, 147.77, 147.97, 168.44, 189.61, 190.01 ppm. HR-MALDI-MS (DHB): calcd

for $C_{33}H_{25}N_3O_6S$ (M)$^+$ 591.14586; found 591.14612. IR (HATR): ν = 2925, 1643,

1555, 1514, 1413, 1334, 1212, 1156, 1105, 1050, 984, 821 cm^{-1}.

Supporting information (SI) available: Experimental procedures and characterization of compounds, DSC analyses, electrochemical data, UV-Vis absorption spectra, DFT calculations, correlations, ^{1}H and ^{13}C NMR spectra, and HR-MALDI-MS spectra.

Acknowledgements

References

1. Forrest, S. R.; Thompson, M. E. *Chem. Rev*. **2007**, *107*, 923−1386.

2. Miller, R. D.; Chandross, E. A. *Chem. Rev*. **2010**, *110*, 1−574.

3. Bureš, F. *RSC Advances* **2014**, *4*, 58826−58851.

4. Kulhánek, J.; Bureš, F.; Opršal, J.; Kuznik, W.; Mikysek, T.; Růžička, A. *Asian J. Org. Chem*., **2013**, *2*, 422−431.

5. Jarowski, P. D.; Mo, Y. *Chem. Eur. J.*, **2014**, *20*, 17214−17221.

6. Meier, H. *Angew. Chem. Int. Ed.*, **2005**, *44*, 2482−2506.

7. Bureš, F.; Pytela, O.; Kivala, M.; Diederich, F. *J. Phys. Org. Chem.*, **2011**, *24*, 274−281.

8. Prasad, P. N.; Williams, D. J. *Introduction to Nonlinear Optical Effects in Molecules and Polymers,* Wiley-VCH, New York, **1991**.

9. Kuzyk, M. G.; Dirk, C. W. *Characterization Techniques and Tabulations for Organic Nonlinear Optical Materials*, Marcel Dekker, New York, **1998**.

10. Suponitsky, K. Y.; Timofeeva, T. V.; Antipin, M. Y. *Russ. Chem. Rev*. **2006**, *75*, 457–496.

11. Mishra, A.; Bäuerle, P. *Angew. Chem. Int. Ed*. **2012**, *51*, 2020–2067.

12. Duan, C.; Huang, F.; Cao, Y. *J. Mater. Chem. C* **2012**, *22*, 10416–10434.

13. Walker, B.; Kim, C.; Nguyen, T.-Q. *Chem. Mater*. **2011**, *23*, 470–482.

14. Liang, M.; Chen, J. *Chem. Soc. Rev*. **2013**, *42*, 3453–3488.

15. Wu, Y.; Zhu, W. *Chem. Soc. Rev*. **2013**, *42*, 2039–2058.

16. Clifford, J. N.; Martínez-Ferrero, E.; Viterisi, A.; Palomares, E. *Chem.Soc. Rev*. **2011**, *40*, 1635–1646.

17. Ohmori, Y. *Laser Photonics Rev*. **2010**, *4*, 300–310.

18. Facchetti, A. *Mater. Today* **2007**, *10*, 28–37.

19. Sirringhaus, H. *Adv. Mater*. **2014**, *26*, 1319–1335.

20. Malachowski, M. J.; Zmija, J. *Opto-Electron. Rev*. **2010**, *18*, 121–136.

21. Pawlicki, M.; Collins, H. A.; Denning, R. G.; Anderson, H. L. *Angew. Chem. Int. Ed*. **2009**, *48*, 3244–3266.

22. He, G. S.; Tan, L.-S.; Zheng, Q.; Prasad, P. N. *Chem. Rev*. **2008**, *108*, 1245–1330.

23. Parthenopoulos, D. A.; Rentzepis, P. M. *Science*, **1989**, *245*, 843–845.

24. Cumpston, B. H.; Ananthavel, S. P.; Barlow, S.; Dyer, D. L.; Ehrlich, J. E.; Erskine, L. L.; Heikal, A. A.; Kuebler, S. M.; Sandy Lee, I.-Y.; McCord-Maughon, D.; Qin, J.; Röckel, H.; Rumi, M.; Wu, X.-L.; Marder, S. R.; Perry, J. W. *Nature*, **1999**, *398*, 51–54.

25. Strickler, J. H.; Webb, W. W. *Opt. Lett*., **1991**, *16*, 1780–1782.

26. Klikar, M.; Jelínková, V.; Růžičková, Z.; Mikysek, T.; Pytela, O.; Ludwig, M.; Bureš, F. *Eur. J. Org. Chem.* **2017**, *2017*, 2764–2779.

27. Moylan, C. R.; Twieg, R. J.; Lee, V. Y.; Swanson, S. A.; Betterton, K. M.; Miller, R. D. *J. Am. Chem. Soc.* **1993**, *115*, 12599–12600.

28. Ledoux, I.; Zyss, J.; Barni, E.; Barolo, C.; Diulgheroff, N.; Quagliotto, P.; Viscardi, G. *Synth. Met.* **2000**, *115*, 213–217.

29. Asiri, A. M. *J. Chem. Soc. Pak.* **2004**, *26*, 57–60.

30. Das, S.; George, M.; Mathew, T.; Asokan, C. V. *J. Chem. Soc. Perkin Trans. 2* **1996**, 731–736.

31. Chou, S.-S. P.; Yu, C.-Y. *Synth. Met.* **2004**, *142*, 259–262.

32. Nakatsuji, S.; Yahiro, T.; Nakashima, K.; Akiyama, S.; Nakazumi, H. *Bull. Chem. Soc. Jpn.* **1991**, *64*, 1641–1647.

33. Gleiter, R.; Hoffmann, H.; Irngartinger, H.; Nixdorf, M. *Chem. Ber.* **1994**, *127*, 2215–2224.

34. Krasnaya, Z. A.; Smirnova, Y. V. *Russ. Chem. Bull.* **1997**, *46*, 2086–2088.

35. Raimundo, J.-M.; Blanchard, P.; Ledoux-Rak, I.; Hierle, R.; Michaux, L.; Roncali, J. *Chem. Commun.* **2000**, 1597–1598.

36. Raimundo, J.-M.; Blanchard, P.; Frère, P.; Mercier, N.; Ledoux-Rak, I.; Hierle, R.; Roncali, J. *Tetrahedron Lett.* **2001**, *42*, 1507–1510.

37. Raimundo, J.-M.; Blanchard, P.; Gallego-Planas, N.; Mercier, N.; Ledoux-Rak, I.; Hierle, R.; Roncali, J. *J. Org. Chem.* **2002**, *67*, 205–218.

38. Andreu, R.; Aramburo, J.; Cerdán, M. A.; Garín, J.; Orduna, J.; Villacampa, B. *Tetrahedron Lett.* **2006**, *47*, 661–664.

39. Stankovic, E.; Toma, S.; Van Boxel, R.; Asselberghs, I.; Persoons, A. *J. Organomet. Chem.* **2001**, *637–639*, 426–434.

40. Janowska, I.; Zakrzewski, J.; Nakatani, K.; Delaire, J. A.; Palusiak, M.; Walak, M.; Scholl, H. *J. Organomet. Chem.* **2003**, *675*, 35–41.

41. Janowska, I.; Zakrzewski, J.; Nakatani, K.; Palusiak, M.; Walak, M.; Scholl, H. *J. Organomet. Chem.* **2006**, *691*, 323–330.

42. Alain, V.; Blanchard-Desce, M.; Chen, C.-T.; Marder, S. R.; Fort, A.; Barzoukas, M. *Synth. Met.* **1996**, *81*, 133–136.

43. Borbone, F.; Carella, A.; Ricciotti, L.; Tuzi, A.; Roviello, A.; Barsella, A. *Dyes Pigm.* **2011**, *88*, 290–295.

44. El-Shishtawy, R. M.; Borbone, F.; Al-Amshany, Z. M.; Tuzi, A.; Barsella, A.; Asiri, A. M.; Roviello, A. *Dyes Pigm.* **2013**, *96*, 45–51.

45. Seniutinas, G.; Tomašiünas, R.; Czaplicki, R.; Sahraoui, B.; Daškevičiene, M.; Getautis, V.; Balevičius, Z. *Dyes Pigm.* **2012**, *95*, 33–40.

46. Traskovskis, K.; Mihailovs, I.; Tokmakovs, A.; Jurgis, A.; Kokars, V.; Rutkis, M. *J. Mater. Chem.* **2012**, *22*, 11268–11276.

47. Hao, Y.; Yang, X.; Cong, J.; Tian, H.; Hagfeldt, A.; Sun, L. *Chem. Commun.* **2009**, 4031–4033.

48. Bürckstümmer, H.; Tulyakova, E. V.; Deppish, M.; Lenz, M. R.; Kronenberg, N. M.; Gsänger, M.; Stolte, M.; Meerholz, K.; Würthner, F. *Angew. Chem. Int. Ed.* **2011**, *50*, 11628–11632.

49. Roquet, S.; Cravino, A.; Leriche, P.; Alévque, O.; Frère, P.; Roncali, J. *J. Am. Chem. Soc.* **2006**, *128*, 3459–3466.

50. Hirade, M.; Yasuda, T.; Adachi, C. *J. Phys. Chem. C* **2013**, *117*, 4986–4991.

51. Planells, M.; Robertson, N. *Eur. J. Org. Chem.* **2012**, 4947–4953.

52. Xiao, J.; Deng, Z.-B.; Yao, Y.-S.; Wang, X.-S. *Dyes Pigm.* **2008**, *76*, 290–293.

53. Kumar, N. S. S.; Varghese, S.; Narayan, G.; Das, S. *Angew. Chem. Int. Ed.* **2006**, *45*, 6317–6321 or *Angew. Chem.* **2006**, *118*, 6465−6469.

54. Kumar, N. S. S.; Abraham, S.; Ratheesh, K. V.; Tamaoki, N.; Furumi, S.; Das, S. *J. Photochem. Photobiol. A: Chemistry* **2009**, *207*, 73–78.

55. Lv, Y.; Guo, Y.; Xu, J.; Shao, S. *J. Fluorine Chem.* **2011**, *132*, 973–977.

56. Citterio, D.; Sasaki, S.-I.; Suzuki, K. *Chem. Lett.* **2001**, *30*, 552–553.

57. Ahmedova, A.; Burdzhiev, N.; Cattini, S.; Stanoeva, E.; Mitewa, M. *C. R. Chim.* **2010**, *13*, 1269–1277.

58. Klikar, M.; Solanke, P.; Tydlitát, J.; Bureš, F. *Chem. Rec.* **2016**, *16*, 1886−1905.

59. Solanke, P.; Bureš, F.; Pytela, O.; Kulhánek, J.; Padělková, Z. *Synthesis* **2013**, 3044−3051.

60. Solanke, P.; Bureš, F.; Pytela, O.; Klikar, M.; Mikysek, T.; Mager, L.; Barsella, A.; Růžičková, Z. *Eur. J. Org. Chem.* **2015**, 5339−5349.

61. Adhikari, T.; Solanke, P.; Pathak, D.; Wágner, T.; Bureš, F.; Reed, T.; Nunzi, J.-M. *Opt. Mater.* **2017**, *69*, 312−317.

62. Solanke, P.; Růžička, A.; Mikysek, T.; Pytela, O.; Bureš, F.; Klikar, M. *Helv. Chim. Acta* **2018**, *101*, e201800090 (1−13).

63. Isse, A. A.; Gennaro, A. *J. Phys. Chem. B*, **2010**, *114*, 7894−7899.

64. Sawyer, D. T.; Sobkowiak, A.; Roberts, J. L. *Electrochemistry for Chemists, 2nd edition*, J. Wiley and Sons Inc., **1995**.

65. Gaussian 16, Revision A.03, M. J. Frisch, G. W. Trucks, H. B. Schlegel, G. E. Scuseria, M. A. Robb, J. R. Cheeseman, G. Scalmani, V. Barone, G. A. Petersson, H. Nakatsuji, X. Li, M. Caricato, A. V. Marenich, J. Bloino, B. G. Janesko, R. Gomperts, B. Mennucci, H. P. Hratchian, J. V. Ortiz, A. F. Izmaylov, J. L. Sonnenberg, D. Williams-Young, F. Ding, F. Lipparini, F. Egidi, J. Goings, B.

Peng, A. Petrone, T. Henderson, D. Ranasinghe, V. G. Zakrzewski, J. Gao, N. Rega, G. Zheng, W. Liang, M. Hada, M. Ehara, K. Toyota, R. Fukuda, J. Hasegawa, M. Ishida, T. Nakajima, Y. Honda, O. Kitao, H. Nakai, T. Vreven, K. Throssell, J. A. Montgomery, Jr., J. E. Peralta, F. Ogliaro, M. J. Bearpark, J. J. Heyd, E. N. Brothers, K. N. Kudin, V. N. Staroverov, T. A. Keith, R. Kobayashi, J. Normand, K. Raghavachari, A. P. Rendell, J. C. Burant, S. S. Iyengar, J. Tomasi, M. Cossi, J. M. Millam, M. Klene, C. Adamo, R. Cammi, J. W. Ochterski, R. L. Martin, K. Morokuma, O. Farkas, J. B. Foresman, and D. J. Fox, Gaussian, Inc., Wallingford CT, **2016**.

66. da S. Oliveira, A. F. C.; de Souza, A. P. M.; de Oliveira, A. S.; da Silva, M. L.; de Oliveira, F. M.; Santos, E. G.; da Silva, Í, E. P.; Ferreira, R. S.; Villela, F. S.; Martins, F. T.; Leal, D. H. S.; Vaz, B. G.; Teixeira, R. R.; de Paula, S. O. *Eur. J. Med. Chem.* **2018**, *149*, 98–109.

67. Davis, R.; Das, S.; George, M.; Druzhinin, S.; Zachariasse, K. A. *J. Phys. Chem. A*, **2001**, *105*, 4790–4798.

Highlights

- Threefold acceptor/donor substitution of central indan-1,3-dione to gain extraordinary T-shaped push-pull chromophores.

- Fundamental thermal and optoelectronic properties studied by differential scanning calorimetry, electrochemistry, UV/Vis absorption spectroscopy, and DFT calculations.

- Thorough structure–property relationships/intramolecular charge-transfer assessment and correlation of the experimental and theoretical data.